Proc. Natl. Acad. Sci. USA
Vol. 93, pp. 8040–8045, July 1996
Neurobiology

Induction of long-term potentiation is associated with major ultrastructural changes of activated synapses

(hippocampus/morphometry/spine/calcium/CA1)

PIERRE-ALAIN BUCHS AND DOMINIQUE MULLER*

Pharmacology, Centre Médical Universitaire, 1211 Geneva 4, Switzerland

Communicated by M. R. Rosenzweig, University of California, Berkeley, CA, April 2, 1996 (received for review July 3, 1995)

ABSTRACT **Long-term potentiation (LTP), an increase in synaptic efficacy believed to underlie learning and memory mechanisms, has been proposed to involve structural modifications of synapses. Precise identification of the morphological changes associated with LTP has however been hindered by the difficulty in distinguishing potentiated or activated from nonstimulated synapses. Here we used a cytochemical method that allowed detection in CA1 hippocampus at the electron microscopy level of a stimulation-specific, D-AP5-sensitive accumulation of calcium in postsynaptic spines and presynaptic terminals following application of high-frequency trains. Morphometric analyses carried out 30–40 min after LTP induction revealed dramatic ultrastructural differences between labeled and nonlabeled synapses. The majority of labeled synapses (60%) exhibited perforated postsynaptic densities, whereas this proportion was only 20% in nonlabeled synaptic contacts. Labeled synaptic profiles were also characterized by a larger apposition zone between pre- and postsynaptic structures, longer postsynaptic densities, and enlarged spine profiles. These results add strong support to the idea that ultrastructural modifications and specifically an increase in perforated synapses are associated with LTP induction in field CA1 of hippocampus and they suggest that a majority of activated contacts may exhibit such changes.**

Long-term potentiation (LTP) is a remarkably stable form of plasticity that, in area CA1 of the hippocampus, crucially depends for its induction upon activation of *N*-methyl-D-aspartate (NMDA) receptors and calcium entry in postsynaptic spines (1, 2). Methods that reveal this calcium accumulation in postsynaptic spines would thus be extremely useful by allowing identification of specific sets of synapses activated by trains of stimulation. At the electron microscopy level, several techniques have been developed to study calcium accumulation in subcellular structures, including precipitation methods (3, 4). Recently, we developed a new cytochemical method that reveals the calcium accumulated in or bound to specific structures under the form of fine electron-dense precipitate. This method was found to be reproducible and specific for calcium (5). In addition, techniques such as energy-loss electron spectroscopy and electron spectroscopy imaging showed that the precipitate does contain calcium (5). Here we used this approach and tested whether it could allow identification of activated versus nonstimulated synapses. The results indicate that it is possible to detect a stimulation-induced, D-AP5-sensitive accumulation of calcium in a subset of synaptic contacts and that, following LTP induction, these labeled synapses exhibit major differences in their ultrastructural characteristics with regard to nonlabeled profiles.

The publication costs of this article were defrayed in part by page charge payment. This article must therefore be hereby marked "*advertisement*" in accordance with 18 U.S.C. §1734 solely to indicate this fact.

MATERIALS AND METHODS

Preparation and Stimulation of Cultures. Organotypic slice cultures prepared from 7-day-old Sivz rats (6) were maintained 10–12 days in culture before being tested in an interface recording chamber and processed for electron microscopy. For stimulation, an electrode made of twisted nichrome wires was placed in the CA3 area and evoked extracellular field potentials recorded in the CA1. To induce LTP and label activated spine profiles, we used theta burst stimulation (TBS) (7), a pattern consisting of five bursts applied at 5 Hz with each burst being composed of four pulses at 100 Hz. To maximize LTP induction, this pattern of stimulation was applied twice at 10-s intervals. In the experiments shown in Fig. 3, this stimulation protocol was used once to induce LTP and 30 min later to relabel the same group of synapses. The low-frequency train paradigm that did not induce LTP consisted of 100 pulses at 10 Hz.

Calcium Precipitation Protocol. At different times after stimulation the cultures were carefully removed from the recording chamber and fixed and processed for electron microscopy as described (5). Briefly, the cultures were rinsed in 0.1 M phosphate buffer (pH 7.4) and fixed overnight at 4°C in a solution of 3% glutaraldehyde in phosphate buffer (0.1 M, pH 7.4). After fixation, the samples were rinsed for 1.5 h in phosphate buffer (4°C, 0.1 M, pH 7.4) and postfixed in a solution prepared freshly and containing 1% OsO_4 and 1.5% potassium chromium-trisoxalate $(K_3Cr(C_2O_4))_3$ (Aldrich; pH 9.5 adjusted with KOH) for 2 h at 4°C. After a short rinse in distilled water adjusted to pH 9.5 with KOH (5 min at 4°C), the samples were dehydrated through an ascending series of ethanol concentrations. Ethanol was then replaced by propylene oxide, the samples were infiltrated through graded propylene oxide–EPON (Fluka) mixtures, and finally embedded in EPON. Ultrathin sections were cut on an LKB ultratome with a diamond knife, collected on water, and mounted on uncoated copper grids (200–300 mesh).

Electron Microscopy Analyses. After staining with uranyl acetate and lead citrate, the sections were analyzed in a Phillips CM10 electron microscope at 80 kV. Three or four sections per culture were usually examined. Synapses were randomly photographed in an area corresponding to the proximal and middle portions of the apical dendritic arborization of CA1 pyramidal neurons. Following postfixation with chromium trisoxalate, small electron-dense precipitates were characteristically observed in subcellular structures implicated in calcium metabolism and storage such as mitochondria, vacuoles, or endoplasmic reticulum. Note that this technique only reveals a bound form of calcium and not free calcium, since precipitate is not found in the extracellular space (5). In postsynaptic spines, precipitates were rarely observed under nonstimulated conditions and, when present, they were systematically found to be associated with reticulum-like tubules

Abbreviations: LTP, long-term potentiation; NMDA, *N*-methyl-D-aspartate; TBS, theta burst stimulation; PSD, postsynaptic density.

*To whom reprint requests should be addressed.

(endoplasmic reticulum or spine apparatus; see Figs. 1 *A* and *D*, 2*A*, 3 *C* and *D*). Curiously these structures were only exceptionally detectable in nonlabeled spines (see Figs. 1 *B* and *C* or 3*B*) as if calcium accumulation and the calcium–trisoxalate–osmium reaction markedly intensified their staining. For quantitative analyses, postsynaptic spine profiles were classified as either labeled or nonlabeled using as the only criteria the presence of accumulated electron-dense precipitates in either of these cytoplasmic structures. To minimize subjectivity, classification was carried out blind by at least two experimenters and if distinction was unclear, the synapse was not included in the quantification. The precipitate density was assessed by digitizing negatives of synapses photographed at a magnification of ×28,500. Using threshold imaging techniques, the precipitate could be revealed due to its marked electron density. Measurements were expressed as the ratio of pixels of precipitate versus those of the profile area.

For morphometric studies, synaptic contacts were randomly selected and photographed at a magnification of ×28,500. These negatives were digitized and morphometric analyses carried out using image analysis and statistical software developed under MATLAB 4.1. To minimize possibilities of bias, analyses were made blind and results were expressed as one averaged value per experiment with n representing the number of slice cultures. Statistical analyses were carried out using the Mann–Whitney test.

RESULTS

To assess whether a precipitation method could be used to identify activated from nonstimulated synapses, we applied TBS to a group of CA3 neurons in hippocampal organotypic cultures and then measured the proportion of spine profiles observed in the CA1 region that contained precipitates (Fig. 1). Under control conditions, i.e. in the absence of stimulation, precipitate was rarely observed in synaptic subcellular structures and only a small proportion of spine profiles (5.3 ± 0.2%; $n = 6$; 610 profiles analyzed) contained electron-dense deposits. Following stimulation, the proportion of spine profiles that contained precipitate markedly increased to 16.2 ± 0.5% 1–2 min after stimulation. This proportion was still 11.8 ± 0.6% after 7 min ($n = 6$; 593 and 363 profiles analysed; $P < 0.001$) and returned to control values after 15 min. The magnitude of these changes was very reproducible and compatible with estimates of the proportion of synapses possibly activated by this type of stimulation (8).

To assess the specificity of this spine labeling, slices were stimulated with trains that were not likely to activate NMDA receptors and did not induce LTP (100 pulses at 10 Hz) or with TBS applied in the presence of the NMDA receptor antagonist D-AP5 (50 μM). Under these two conditions, no influx of calcium in postsynaptic spines was expected and LTP was not induced. As illustrated in Fig. 1*E*, there was also no increase in the number of spine profiles containing calcium deposits (711 and 997 profiles analyzed, respectively).

As an additional test of the selectivity of this labeling technique we investigated whether there was a correlation between the presence of precipitate in postsynaptic spine profiles and in their attached presynaptic terminal. In three experiments, we fixed slices 1–2 min after high-frequency stimulation and measured the mean density of precipitate (Fig. 2 *A* and *B*) found in presynaptic terminal profiles attached to labeled and nonlabeled spines. As illustrated in Fig. 2 *C* and *D*, the mean precipitate density was respectively 3.3 ± 0.2% and 0.9 ± 0.1% in terminals facing labeled and nonlabeled spine profiles ($P < 0.01$) and analysis of the density distribution in presynaptic terminals clearly showed a shift to the right when spine profiles were labeled ($P < 0.05$).

To investigate the ultrastructural correlate of synaptic potentiation, we then carried out a comparative morphometric analysis of labeled versus nonlabeled spine profiles. To obtain an image of synapses at a time when stable LTP was expressed, TBS was applied to a group of CA3 neurons and the enhancement of synaptic efficacy monitored for 30 min in the CA1 area. After 30 min, a second episode of high-frequency stimulation was reapplied to relabel the same group of synapses (Fig. 3*A*). The absence of additional LTP produced by this second theta burst episode indicated that the stimulation most likely activated the same group of synapses. Five minutes after this second episode, organotypic hippocampal cultures were fixed, embedded, and synapses randomly photographed in the CA1 area. Six slices were treated in the same way, and 230 labeled and 246 nonlabeled spine profiles were analyzed using nonserial sections of the tissue.

Major differences were observed between labeled and nonlabeled synapses present within the same sections. A major change concerned spine profiles with perforated postsynaptic densities [defined by the presence of a clear interruption of the postsynaptic density (PSDs); Fig. 3 *C* and *D*]. These perforated profiles were three times more numerous among activated synapses (59.9 ± 2.1% versus 22.7 ± 1.1%; $P < 0.0001$; Fig. 3*E*). This change was very robust and reproducible in the six experiments that we carried out. Significant differences were also observed concerning the area of the spine head profiles (0.38 ± 0.03 versus 0.22 ± 0.02 μm^2; $P < 0.001$; Fig. 3*E*), the length of the PSD profiles (0.79 ± 0.02 versus 0.63 ± 0.04 μm; $P < 0.05$; Fig. 3*E*), and the length of the apposition zone profiles between pre- and postsynaptic structures (1.78 ± 0.05 versus 1.32 ± 0.06 μm; $P < 0.01$; Fig. 3*E*). However, no differences with regard to neck diameter, neck length, or density of presynaptic vesicles were detected (data not shown).

Since a possible bias could have been introduced by the selection of profiles with precipitates, a comparative morphometric analysis of 118 labeled and 135 nonlabeled profiles seen in nonstimulated cultures was also carried out. The results of four experiments showed that the selection of spines containing precipitates did, as suspected, favor slightly larger profiles. This small bias, however, did not account for all changes reported after stimulation. First, the proportion of profiles with perforated PSDs was very similar in these nonstimulated, labeled, and nonlabeled synapses (Fig. 4*A*), thereby indicating that the selection of precipitate-containing profiles did not, per se, affect analyses of the proportion of perforated PSDs. Second, the values of spine head area found after stimulation were still significantly larger than those of labeled profiles seen under control conditions, without stimulation ($P < 0.01$; see Fig. 4*B*).

Another important question was to determine whether the differences observed between labeled and nonlabeled profiles reflected stable changes associated with LTP or modifications possibly related to the stimulation. To address this issue, analyses were also carried out in the experiments performed in the presence of D-AP5 as well as in cultures fixed 1–2 min after the first LTP inducing train. Because no changes in the labeling of postsynaptic spine profiles could be detected in the D-AP5 experiments, we compared the size and number of perforated PSDs of spine profiles facing heavily and poorly labeled presynaptic terminals. This comparison showed a difference in spine head area measurements (0.34 ± 0.02 versus 0.23 ± 0.02 μm^2 for profiles facing labeled and nonlabeled terminals, respectively; $n =$ 71 and 98; $P < 0.01$), but no difference in proportion of perforated PSDs (20 ± 2.9% versus 19 ± 2.1%). Also, in the experiments in which cultures were fixed 1–2 min after the first LTP train, the proportion of spine profiles with perforated PSDs, although slightly increased, was not statistically different at this time point from control values (Fig. 4*A*). Note that the increase in perforation numbers that occurs between 1–2 min and 35 min after LTP induction cannot be related to differences in the size distribution of spine profiles (Fig. 4*B*).

DISCUSSION

The precipitation method used in these experiments revealed a subset of synapses that accumulated precipitate in a stimulation-dependent and D-AP5-sensitive way. Several observations are consistent with the interpretation that a majority of these labeled synapses represented activated synapses. First, the stimulation patterns used are known to trigger an influx of calcium in synaptic structures (1, 2) and previous studies have provided evidence that the precipitate is likely to reflect calcium accumulation in subcellular organelles (5). In agreement with similar or other methods (3, 4), the precipitate was found in structures known to participate in calcium metabolism and electron spectroscopy techniques have demonstrated the presence of calcium within the precipitate (5). Second, accumulation of precipitate in postsynaptic spine profiles was specifically related to the application of LTP-inducing trains and was not observed with the low-frequency stimulation protocol or when TBS was applied in the presence of D-AP5. This D-AP5-sensitivity probably represents the strongest argument supporting a link between the pres-

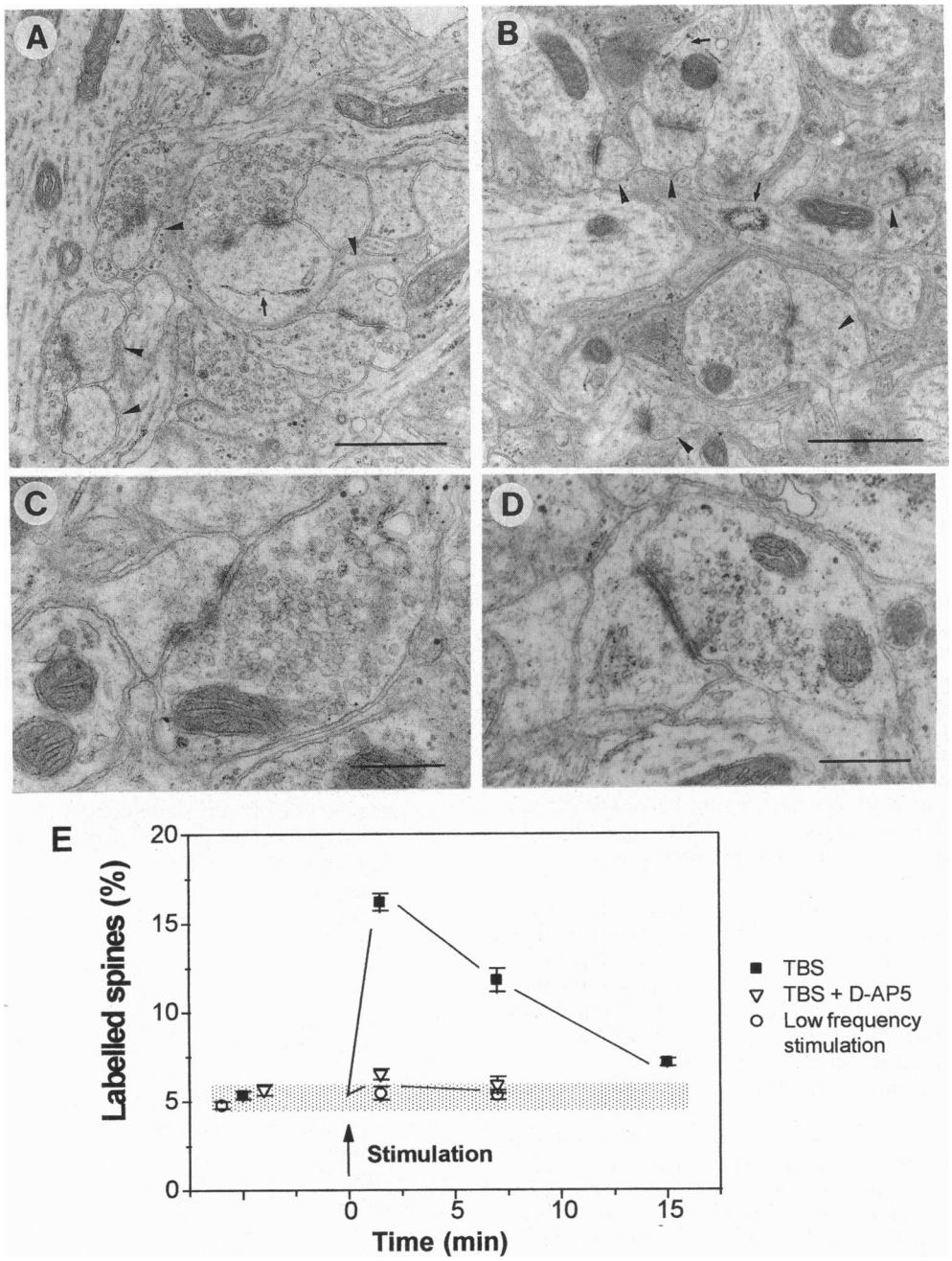

FIG. 1. NMDA receptor-dependent accumulation of precipitate in postsynaptic spine profiles revealed by a cytochemical method. (*A*) Low magnification view of the neuropil of a section through a CA1 hippocampal organotypic culture fixed 5 min after TBS. Note the presence of one markedly labeled spine profile (arrow) among four other unlabeled synapses (arrowheads). In dendritic and synaptic structures, precipitate, when present, was characteristically observed in reticulum-like tubules and mitochondria. (Bar = 1 μm.) (*B*) View of the neuropil (CA1) of a culture fixed 15 min after stimulation. Precipitate is much less frequently observed, but is still detectable in a few dendritic and axonal structures (arrows). However, most spine profiles (arrowheads) appear at that time as unlabeled. (Bar = 1 μm.) (*C* and *D*) Higher magnification view of a nonlabeled (*C*) and labeled (*D*) synapse observed in a culture fixed 7 min after stimulation. (Bars = 0.5 μm.) (*E*) Changes in the proportion of labeled spine profiles observed in organotypic cultures fixed at different times after TBS (arrow; ■), TBS applied in the presence of 50 μM D-AP5 (Δ) or low-frequency stimulation (100 pulses at 10 Hz; ○). Each point represents a mean ± SEM of the analysis of 363–610 synaptic contacts obtained in sections of 3–6 individual cultures. The changes observed 1 and 7 min after LTP-inducing trains are highly significant ($P < 0.001$; Mann–Whitney and Student's *t* test).

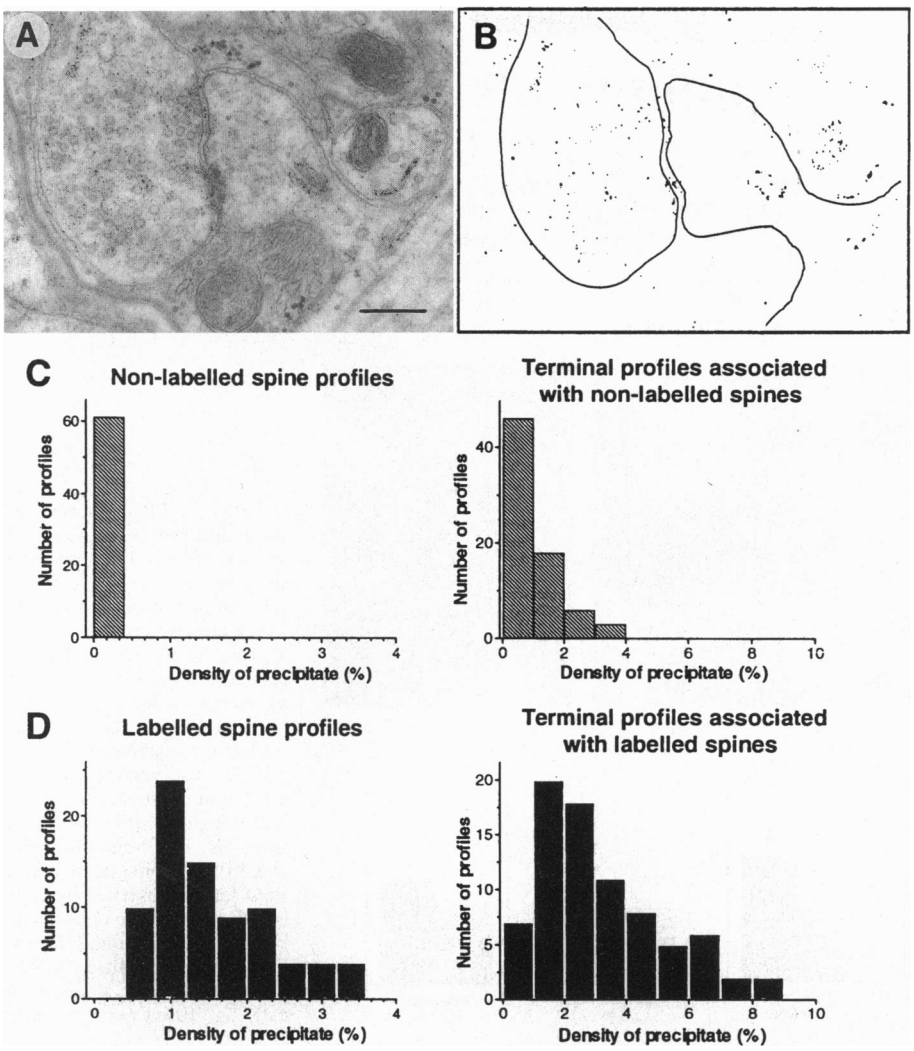

FIG. 2. The stimulation-induced accumulation of precipitate in postsynaptic spine profiles is associated with an enhanced labeling of the attached presynaptic terminal. (*A*) Illustration of a labeled synapse observed in a slice culture fixed 1–2 min after high-frequency stimulation. (*B*) Precipitate detected in the same synapse by threshold imaging techniques (synaptic contour drawn by hand). (*C*) Distribution of the precipitate density found in 78 nonlabeled spine profiles (*left*) and their attached presynaptic terminal (*right*). (*D*) Distribution of the precipitate density found in 83 labeled spine profiles (*left*) and their attached presynaptic terminal (*right*). The precipitate distributions found in terminals associated with labeled and nonlabeled spine profiles are statistically significantly different ($P < 0.05$).

ence of precipitate in spine profiles and the application of high-frequency stimulation. Finally the good correlation observed between pre- and postsynaptic labeling further supports the contention that the NMDA receptor-dependent accumulation of precipitate in spine profiles required activation of the presynaptic terminal. Taken together, these results strongly argue for the interpretation that a majority of the labeled synapses revealed after stimulation by this precipitation method represented activated synapses.

The second important result of the study is that labeled synapses observed after LTP induction markedly differed from nonlabeled contacts. The major difference concerned the proportion of synapses with perforated PSDs, but a difference in size between control and labeled spine profiles was also detected (Fig. 4*B*).

Interpretation of these results must take into consideration the following two issues. First, these data were obtained by analyzing single, nonserial ultrathin sections of stimulated tissue, an approach that may introduce biases. There is evidence, for example, that analyses without partial or complete serial reconstruction lead to an underestimation of the number of perforated contacts (9). Also, without unbiased stereological techniques, factors such as the thickness of ultrathin sections, truncation and overprojection effects, and shrinkage of the tissue during processing may significantly alter quantitative analyses of morphological structures (10). These biases could have affected the numbers reported here, although it seems unlikely that they would modify the major conclusion of the study, since the underestimation of perforated contacts would probably concern both control and stimulated synapses and because these biases are unlikely to account for the 3-fold increase in perforated synapses detected after LTP induction.

Second, is the possibility that the stimulation–precipitation method used here simply reveals larger synapses and may have thus affected numbers of perforated synapses. This seems unlikely for three reasons. (*i*) No changes in the number of labeled spine profiles were detected in the D-AP5 experiments, although the profiles associated with labeled presynaptic terminals were enlarged. This further supports the contention that the stimulation–precipitation method reveals synapses in which NMDA receptors have been activated and not simply larger synapses. (*ii*) Comparisons of the proportion of perforated synapses under control conditions in labeled and nonlabeled profiles indicates that the selection of precipitate-containing spines does not significantly affect perforation

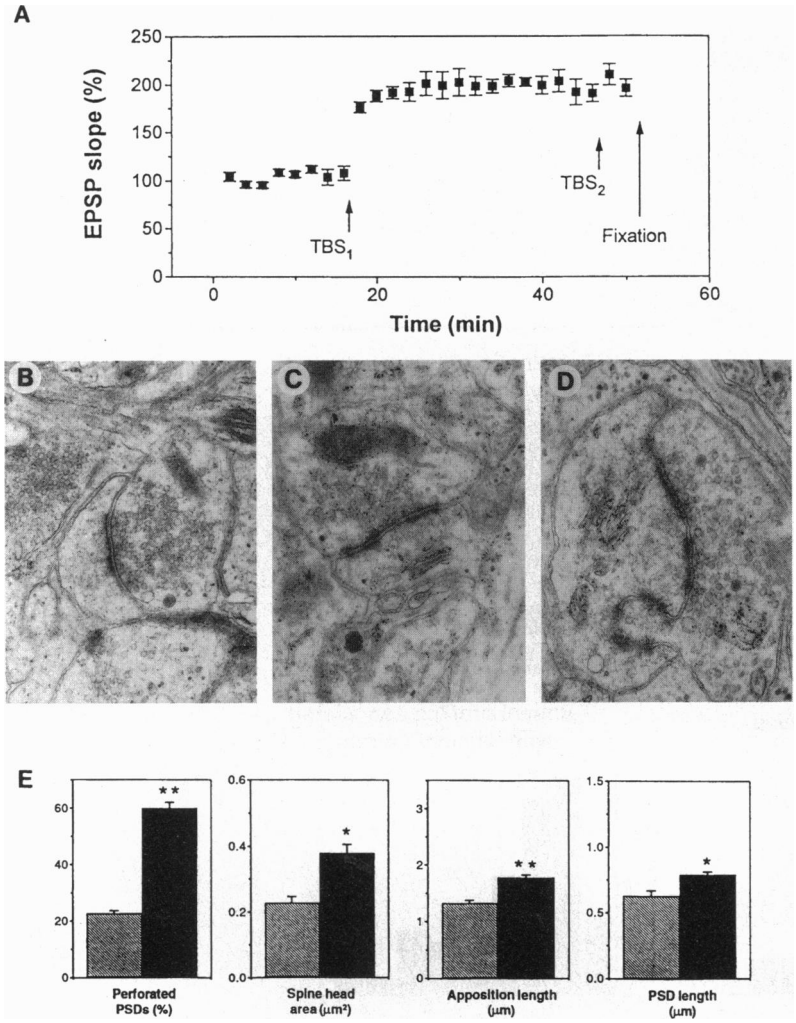

FIG. 3. LTP induction results in major ultrastructural differences between labeled and nonlabeled spine profiles. (*A*) Electrophysiological recording of the changes in synaptic efficacy observed following LTP induction in six organotypic cultures processed for electron microscopy analysis. TBS was applied to a group of CA3 neurons to induce LTP and then repeated 30 min later at a time when LTP was stable to relabel the same group of synapses. Cultures were then fixed 5 min later. (*B–D*) Illustration of representative nonlabeled (*B*) and labeled (*C* and *D*) spine profiles observed within the same cultures following LTP induction. Note the presence of sometimes multiple perforations in labeled profiles. (Bar = 0.5 μm.) (*E*) Differences in spine profiles with perforated PSDs, spine head area, apposition length, and PSD length observed by comparison of 230 nonlabeled (crosshatched bars) and 246 labeled (solid bars) profiles obtained from six cultures. Results are expressed as mean ± SEM of the average value obtained for each slice. All differences are statistically significant (**, $P < 0.001$ and *, $P < 0.01$).

numbers. (*iii*) The proportion of perforated synapses was found to be increased only 35 min, and not 1–2 min, after LTP induction, although under both conditions labeled spine profiles were characterized by the same size distribution (Fig. 4*B*). Taken together, these observations support the interpretation that the 3-fold increase in perforated synapses observed 35 min after high frequency stimulation is related to LTP induction and not to a possible bias introduced by the stimulation–precipitation method or by stimulation-induced changes in size of synaptic structures.

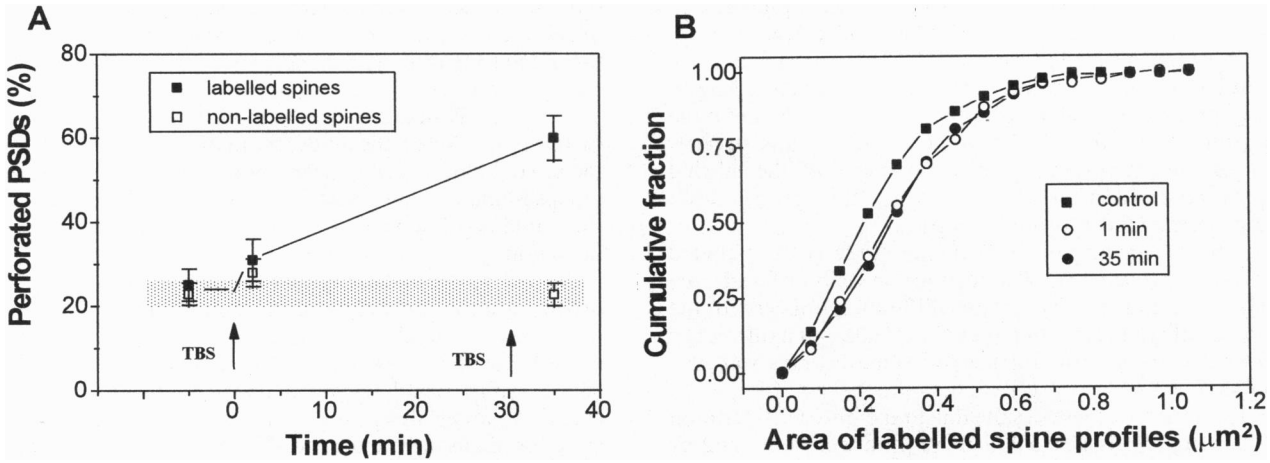

FIG. 4. Time course of the changes in the number of perforated synapses and the spine profile area observed following LTP induction. (*A*) Changes in the proportion of spine profiles with perforated PSDs seen under control conditions, 1–2 min and 35 min after LTP induction in labeled (■) and nonlabeled (□) spine profiles. Results are expressed as mean ± SEM of the values obtained in each slice. (*B*) Cumulative histogram of the measurements of spine head area of the labeled profiles represented in *A* under nonstimulated conditions (control, ■) and at time 1–2 min (○) and 35 min (●) after LTP induction. The shift to the right of the cumulative distributions obtained after stimulation is statistically significant ($P < 0.01$).

This conclusion is in agreement with and confirms several other reports (9, 11–14) and is also consistent with results obtained by serial reconstruction of spines in area CA1 (15, 16). The surprising aspect of these results, however, is the magnitude of the changes that have been observed. Considering the increase in profiles with perforated PSDs, and the background labeling obtained under control conditions, it would seem that 60–80% of activated synapses became perforated spine contacts following LTP induction. Whether this ratio relates to the proportion of potentiated synapses among activated ones remains to be established.

In view of the changes reported here, it is tempting to propose that these ultrastructural modifications contribute to the enhancement of synaptic efficacy that underlies LTP. The increased proportion of perforated contacts, the changes in apposition zone, and PSD length are parameters that may very well affect synaptic efficacy either by enhancing postsynaptic sensitivity or increasing the number of releasing sites. These modifications could account for the puzzling observations indicating that LTP is associated with changes in both quantal size and quantal content of synaptic responses (17, 18). Also, the present results are consistent with recent evidence implicating molecules susceptible to affect cell-to-cell interactions or cell shape in LTP (19, 20), and they support the interpretation that defined structural changes may be generated by specific patterns of activity in the brain (9, 11, 21–23).

We wish to thank L. Stoppini and L. Parisi for preparing the organotypic cultures and for excellent technical assistance, P. Corrèges for his contribution to the development of the image analysis software. This work was supported by Fonds National de la Recherche Scientifique Grants 31-30980.91 and 3100-040815.94 and the De Reuter Foundation.

1. Lynch, G., Larson, J., Kelso, S., Barrionuevo, G. & Schottler, F. (1983) *Nature (London)* **305,** 719–721.
2. Malenka, R. C., Kauer, J. A., Zucker, R. J. & Nicoll, R. A. (1988) *Science* **242,** 81–84.
3. Andrews, S. B., Leapman, R. D., Landis, D. M. D. & Reese, T. S. (1987) *Proc. Natl. Acad. Sci. USA* **84,** 1713–1717.
4. Fifkova, E., Markham, J. A. & Delay, R. (1983) *Brain Res.* **266,** 163–169.
5. Buchs, P.-A., Stoppini, L., Parducz, A., Siklos, L. & Muller, D. (1994) *J. Neurosci. Methods* **54,** 83–93.
6. Stoppini, L., Buchs, P.-A. & Muller, D. (1991) *J. Neurosci. Methods* **37,** 173–182.
7. Larson, J. & Lynch, G. (1986) *Science* **232,** 985–987.
8. Anderson, P. (1990) *Prog. Brain Res.* **83,** 215–222.
9. Geinisman, Y., DeToledo-Morrell, L. & Morrell, F. (1991) *Brain Res.* **566,** 77–88.
10. Gundersen, R. (1986) *J. Microsc.* **143,** 3–45.
11. Greenough, W. T., West, R. W. & De Voogd, T. J. (1978) *Science* **202,** 1096–1098.
12. Schuster, T., Krug, M. & Wenzel, J. (1990) *Brain Res.* **523,** 171–174.
13. Geinisman, Y., DeToledo-Morrell, L., Morrell, F., Heller, R. E., Rossi, M. & Parshall, R. F. (1993) *Hippocampus* **3,** 435–446.
14. Trommald, M., Vaaland, J. L., Blackstad, T. W. & Andersen P. (1990) in *Neurotoxicity of Excitatory Amino Acids*, eds. Guidotti, A. & Costa, E. (Raven, New York), pp. 163–174.
15. Harris, K. M., Jensen, F. E. & Tsao, B. (1992) *J. Neurosci.* **12,** 2685–2695.
16. Sorra, K. E. & Harris, K. M. (1993) *J. Neurosci.* **13,** 3736–3743.
17. Kullmann, D. M. & Nicoll, R. A. (1992) *Nature (London)* **357,** 240–244.
18. Liao, D., Jones, A. & Malinow, R. (1992) *Neuron* **9,** 1089–1097.
19. Mayford, M., Barzilai, A., Keller, F., Schacher, S. & Kandel, E. R. (1992) *Science* **256,** 638–644.
20. Lüthi, A., Laurent, J.-P., Figurov, A., Muller, D. & Schachner, M. (1994) *Nature (London)* **372,** 777–779.
21. Glanzman, D. L., Kandel, E. R. & Schacher, S. (1990) *Science* **249,** 799–802.
22. Bailey, C. H. & Kandel, E. R. (1993) *Annu. Rev. Physiol.* **55,** 397–426.
23. Harris, K. M. & Kater, S. B. (1994) *Annu. Rev. Neurosci.* **17,** 341–371.